

Experimental Test of Einstein-Podolsky-Rosen Paradox and its Generated Steering Inequality

Tianfeng Feng,¹ Changliang Ren,^{2,*} Qin Feng,¹ Maolin Luo,¹ Xiaogang Qiang,³ Jing-Ling Chen,^{4,†} and Xiaoqi Zhou^{1,‡}

¹State Key Laboratory of Optoelectronic Materials and Technologies and School of Physics, Sun Yat-sen University, Guangzhou, People's Republic of China

²Center of Quantum information, Chongqing Institute of Green and Intelligent Technology, Chinese Academy of Sciences, People's Republic of China

³National Innovation Institute of Defense Technology, AMS, Beijing, China

⁴Theoretical Physics Division, Chern Institute of Mathematics, Nankai University, Tianjin 300071, People's Republic of China

(Dated: April 24, 2022)

The Einstein-Podolsky-Rosen (EPR) paradox is the earliest quantum paradox, which was motivated by the fundamental problem whether local realism can completely describe quantum mechanics. The EPR paradox has stimulated an important concept of “quantum nonlocality”, which is classified into three distinct types: entanglement, quantum steering, and Bell’s nonlocality. As two well-known quantum paradoxes for Bell’s nonlocality, the Greenberger-Horne-Zeilinger paradox and the Hardy paradox have been well studied and also confirmed in experiments, however, the experimental test of the EPR paradox has not yet been reported. The EPR paradox is essentially a paradox for quantum steering. Very recently, the EPR paradox has been mathematically formulated to a contradiction equality “ $k = 1$ ”, thus rendering its possibility to be directly observed in the experiment. In this work, we perform the first experimental test for the EPR paradox in a two-qubit scenario. Furthermore, by starting from the EPR paradox we can generate the generalized linear steering inequalities, which have an advantage over the usual ones by detecting more steerability of quantum states. Meanwhile, we also perform an experiment to confirm this merit. Within the experimental errors, the experimental results coincide with the theoretical predictions. Our results deepen the understanding of quantum foundations.

Introduction.—Undoubtedly, quantum paradox is an intuitive way to reveal the essential difference between quantum mechanics and classical theory. Among these paradoxes, there are the famous Einstein-Podolsky-Rosen (EPR) paradox [1], the Greenberger-Horne-Zeilinger (GHZ) paradox [2], the Hardy paradox [3], and so on. In 1935, Einstein, Podolsky and Rosen proposed a profound thought-experiment concerning the EPR paradox, which indicated the conflict between local realism and quantum mechanics, thus triggering the investigation of nonlocal properties of quantum entangled states. In the same year, Schrödinger made an immediate response to the EPR’s argument, he introduced a term “steering” to depict “the spooky action at a distance” that was mentioned in the EPR paper [4]. According to Schrödinger, “steering” reflects a kind of nonlocal phenomenon, in a bipartite scenario it describes an ability of one party, say Alice, to prepare the other party (say Bob) particle with different quantum states by simply measuring her own particle with different settings. However, the notion of steering has not been gained much attention and development until the year 2007, when Wiseman *et al.* gave a rigorous definition of it through the quantum information task [5].

Different from Schrödinger, Bell made a distinct response to the EPR paradox by presenting Bell’s nonlocality [6]. In 1964, Bell figured out that some quantum entangled states may indeed violate Bell’s inequality, which hold for any local-hidden-variable (LHV) model. This fact indicates that LHV models cannot completely reproduce all of the quantum predictions, and the violations of Bell’s inequality by entangled states directly imply that the specific quantum states may possess a kind of nonlocal properties – Bell’s nonlocality. Since then, Bell’s nonlocality has been achieved a rapid and fruit-

ful development in two directions [7]: (i) On one hand, some researchers have proposed various kinds of Bell’s inequalities to detect Bell’s nonlocality in different physical systems, for examples, the Clauser-Horne-Shimony-Holt (CHSH) inequality for two qubits [8], the Mermin-Ardehali-Belinskii-Klyshko inequality for multipartite qubits [9], the Collins-Gisin-Linden-Masser-Popescu inequality for two qudits (two d -dimensional quantum systems) [10]. (ii) On the other hand, some researchers have presented the all-versus-nothing (AVN) proof to reveal Bell’s nonlocality without inequality, for which the typical examples are the GHZ paradox and the Hardy paradox. Experimental verifications of Bell’s nonlocality have also been carried out, for instances, Aspect *et al.* has successfully made the first observation of Bell’s nonlocality with the CHSH inequality [11], Pan *et al.* have tested the three-qubit GHZ paradox in the photon-based experiment [12], Torgerson *et al.* have demonstrated the original Hardy paradox [14], and very recently Luo *et al.* have tested the generalized Hardy paradox for the multi-qubit systems [15].

So far, many experiments have been performed to demonstrate the GHZ paradox as well as the Hardy paradox. However, it is seldom heard that the EPR paradox has been tested in experiments, although it is the earliest quantum paradox that appeared in the literature. There are probably two main reasons: (i) The original EPR state $\Psi(x_1, x_2) = \int_{-\infty}^{+\infty} e^{ip(x_1-x_2+x_0)/\hbar}$ is an entangled state in the bipartite continuous-variable system, which is very difficult to prepare in the lab. (ii) The “paradox” in the EPR paradox is not very clear in its mathematical formalism, this results in that people do not know what they should observe or measure in the experiments. As for the GHZ paradox, it can be formu-

lated as a contradiction equality “+1 = -1”, where “+1” represents the prediction of LHV model, while “-1” is the quantum prediction. Thus, if people observed the value of “-1” by some quantum technologies in the practical experiment, then the GHZ paradox was demonstrated. Similarly, the mathematical formalism of the Hardy paradox is as follows: under some certain Hardy-type constraints for probabilities $P_1 = P_2 = \dots = P_N = 0$, the LHV model gives the zero-probability prediction (i.e., $P_{\text{suc}} = 0$), while quantum prediction is $P_{\text{suc}} > 0$, here P_{suc} is the success probability of a specific event. Therefore, by successfully measuring the desired non-zero success probability in the lab under the required Hardy constraints, one may say that he has verified the Hardy paradox.

The purpose of this Letter is two-fold: (i) We shall perform the first experiment to test the EPR paradox in the version of the two-qubit entangled state, instead of the continuous-variable state $\Psi(x_1, x_2)$. The experiment is based on the theoretical result presented in [16], where the researchers have pointed out that the EPR paradox is essentially a steering paradox, and have also mathematically formulated the paradox into a contradiction equality “ $k = 1$ ” for the k -setting steering scenario. (ii) Any quantum paradox can correspond to an inequality, e.g., one can transform the two-qubit Hardy paradox into the well-known CHSH inequality [17][18]. Accordingly, we shall generate a novel steering inequality from the EPR paradox. This inequality is called the generalized linear steering inequality (GLSI), which naturally includes the linear steering inequality as a special case. Theoretically, the GLSI is more powerful in detecting the steerability of pure states and some mixed states. Meanwhile, in this work we also experimentally test quantum violations of the GLSI.

The EPR paradox as a steering paradox “ $k = 1$ ”.—In 2007, Wiseman *et al.* have classified quantum nonlocality into three different types: quantum entanglement, EPR steering, and Bell’s nonlocality [5]. By presenting the steering paradox “ $k = 1$ ”, Ref. [16] has confirmed that EPR steering is exactly the type of quantum nonlocality inherited in the EPR paradox. Following Ref. [16], let us consider an arbitrary two-qubit pure entangled state $\rho_{AB} = |\Psi(\alpha, \varphi)\rangle\langle\Psi(\alpha, \varphi)|$ shared by Alice and Bob. In the Schmidt decomposition, i.e., in the \hat{z} -direction representation, the wave-function $|\Psi(\alpha, \varphi)\rangle$ can be written as follows:

$$|\Psi(\alpha, \varphi)\rangle = \cos \alpha |00\rangle + e^{i\varphi} \sin \alpha |11\rangle, \quad (1)$$

with $\alpha \in (0, \pi/2)$, $\varphi \in [0, 2\pi]$. However, for the same $|\Psi\rangle$, in the general \hat{n} -direction decomposition one may recast it to

$$|\Psi\rangle = |+\hat{n}\rangle|\chi_{+\hat{n}}\rangle + |-\hat{n}\rangle|\chi_{-\hat{n}}\rangle, \quad (2)$$

where $|\pm \hat{n}\rangle$ are the eigenstates of the operator $\hat{P}_a^{\hat{n}}$. Here $\hat{P}_a^{\hat{n}} = [\mathbb{1} + (-1)^a \vec{\sigma} \cdot \hat{n}]/2$ denotes Alice’s projective measurement on her qubit along the \hat{n} -direction with measurement outcomes a ($a = 0, 1$), $\mathbb{1}$ is the identity matrix, $\vec{\sigma} = (\sigma_x, \sigma_y, \sigma_z)$ is the Pauli matrices vector, and $|\chi_{\pm \hat{n}}\rangle = \langle \pm \hat{n} | \Psi(\alpha, \varphi) \rangle$ are the collapsed pure states (unnormalized) for Bob’s qubit.

After Alice performs a projective measurement on her qubit along the \hat{n} -direction, then due to the wave-function collapse she will steer Bob’s qubit to the following pure states $\rho_a^{\hat{n}} = \tilde{\rho}_a^{\hat{n}}/\text{tr}(\tilde{\rho}_a^{\hat{n}})$ with the probability $\text{tr}(\tilde{\rho}_a^{\hat{n}})$, here $\tilde{\rho}_a^{\hat{n}} = \text{tr}_A[(\hat{P}_a^{\hat{n}} \otimes \mathbb{1}) \rho_{AB}]$ are the so-called Bob’s unnormalized conditional states and $\rho_a^{\hat{n}}$ are the normalized ones [5]. The pure entangled state $|\Psi\rangle$ has a remarkable property: Bob’s normalized conditional states are always *pure*, and $\rho_a^{\hat{n}_1} \neq \rho_a^{\hat{n}_2}$ if $\hat{n}_1 \neq \hat{n}_2$. In a two-setting steering protocol $\{\hat{z}, \hat{x}\}$, if Bob’s four unnormalized conditional states can be simulated by an ensemble $\{\wp_\xi \rho_\xi\}$ of the local-hidden-state (LHS) model, then they can be only described as (see Supplementary Information [19])

$$\tilde{\rho}_0^{\hat{z}} = \cos^2 \alpha |0\rangle\langle 0| = \wp_1 \rho_1, \quad (3a)$$

$$\tilde{\rho}_1^{\hat{z}} = \sin^2 \alpha |1\rangle\langle 1| = \wp_2 \rho_2, \quad (3b)$$

$$\tilde{\rho}_0^{\hat{x}} = (1/2)|\chi_+\rangle\langle\chi_+| = \wp_3 \rho_3, \quad (3c)$$

$$\tilde{\rho}_1^{\hat{x}} = (1/2)|\chi_-\rangle\langle\chi_-| = \wp_4 \rho_4, \quad (3d)$$

with $|\chi_{\pm}\rangle \equiv |\chi_{\pm \hat{x}}\rangle/\sqrt{\text{tr}[|\chi_{\pm \hat{x}}\rangle\langle\chi_{\pm \hat{x}}|]} = \cos \alpha |0\rangle \pm e^{i\varphi} \sin \alpha |1\rangle$ being the normalized pure states, ρ_i ’s the hidden states, \wp_i ’s the corresponding probabilities appeared in the ensemble, which satisfied the constraint of $\sum_\xi \wp_\xi \rho_\xi = \rho_B = \text{tr}_A[\rho_{AB}]$, here ρ_B is the reduced density matrix of Bob. However, for Eq. (3), due to the relations $\tilde{\rho}_0^{\hat{z}} + \tilde{\rho}_1^{\hat{z}} = \rho_B$ and $\text{tr} \rho_B = 1$, by summing them up and taking trace, the left-hand side and the right-hand side of which will lead to the sharp contradiction “2=1”. This is just the simple steering paradox in the two-setting steering protocol.

The more general steering paradox “ $k = 1$ ” can be similarly obtained if one considers the k -setting steering scenario $\{\hat{n}_1, \hat{n}_2, \dots, \hat{n}_k\}$, where Alice performs k projective measurements on her qubit along \hat{n}_j -directions (with $j = 1, 2, \dots, k$). For each projective measurement $\hat{P}_a^{\hat{n}_j}$, Bob will obtain the corresponding unnormalized pure states as $\tilde{\rho}_a^{\hat{n}_j}$. Suppose these states can be simulated by the LHS model, then one will have the following equation-group containing $2k$ equations [19]:

$$\tilde{\rho}_0^{\hat{n}_j} = \sum_\xi \wp(0|\hat{n}_j, \xi) \wp_\xi \rho_\xi, \quad (4a)$$

$$\tilde{\rho}_1^{\hat{n}_j} = \sum_\xi \wp(1|\hat{n}_j, \xi) \wp_\xi \rho_\xi, \quad (j = 1, 2, \dots, k). \quad (4b)$$

Because all $\tilde{\rho}_a^{\hat{n}_j}$ ’s are proportional to the pure states, thus in the right-hand side of Eq. (4) each summation will finally keep only one ρ_ξ , as the case in Eq. (3). Furthermore, due to $\tilde{\rho}_0^{\hat{n}_j} + \tilde{\rho}_1^{\hat{n}_j} = \rho_B$ and $\sum_{\xi=1}^{2k} \wp_\xi \rho_\xi = \rho_B$, by taking trace of Eq. (4), the left-hand-side gives the quantum prediction as k , and the right-hand side gives the LHV-model prediction as 1, thus yielding the steering paradox “ $k = 1$ ”.

Experimentally, we shall test the EPR paradox with the simplest case of $k = 2$. To do that, we need to perform some measurements to obtain four quantum probabilities. The first one is $P_1^{\text{QM}} = \text{tr}[\tilde{\rho}_0^{\hat{z}} |0\rangle\langle 0|] = \cos^2 \alpha$, which

is obtained from Bob by performing the projective measurement $|0\rangle\langle 0|$ on his unnormalized conditional state as in Eq. (3a). Similarly, from Eq. (3b)-Eq. (3d), one has $P_2^{\text{QM}} = \text{tr}[\hat{\rho}_1^{\hat{z}} |1\rangle\langle 1|] = \sin^2 \alpha$, $P_3^{\text{QM}} = \text{tr}[\hat{\rho}_0^{\hat{x}} |\chi_+\rangle\langle \chi_+|] = 1/2$, and $P_4^{\text{QM}} = \text{tr}[\hat{\rho}_1^{\hat{x}} |\chi_-\rangle\langle \chi_-|] = 1/2$. Consequently, the total quantum prediction is given by $P_{\text{total}}^{\text{QM}} = \sum_{i=1}^4 P_i^{\text{QM}} = 2$, which contradicts with the LHS-model prediction “1”. Therefore, within the experimental measurement errors, if one can obtain the value $P_{\text{total}}^{\text{QM}}$ closing to 2, then he will demonstrate the EPR paradox “2 = 1” in the two-qubit system.

Generalized linear steering inequality.—It is known that Bell’s inequalities can be derived from the GHZ and Hardy paradoxes [17][18]. This is also the case for the EPR paradox. Actually, starting from the steering paradox “ $k = 1$ ”, one can naturally derive a k -setting generalized linear steering inequality. The derivation procedure is as follows: In the steering scenario $\{\hat{n}_1, \hat{n}_2, \dots, \hat{n}_k\}$, Alice performs k projective measurements on her qubit along \hat{n}_j -directions. Based on the two-qubit pure state $|\Psi(\theta, \phi)\rangle$ (note that it is not $|\Psi(\alpha, \varphi)\rangle$), for each measurement $\hat{P}_a^{\hat{n}_j}$, Bob may have the corresponding normalized pure states as $\rho_a^{\hat{n}_j}(\theta, \phi) = \tilde{\rho}_a^{\hat{n}_j} / \text{tr}(\tilde{\rho}_a^{\hat{n}_j})$, here $\tilde{\rho}_a^{\hat{n}_j} = \text{tr}_A[(\hat{P}_a^{\hat{n}_j} \otimes \mathbb{1}) |\Psi(\theta, \phi)\rangle\langle \Psi(\theta, \phi)|]$ with $(a = 0, 1)$. Then the k -setting GLSI can be constructed as follows [19]

$$\mathcal{S}_k(\theta, \phi) = \sum_{j=1}^k \left(\sum_{a=0}^1 P(A_{n_j} = a) \langle \rho_a^{\hat{n}_j} \rangle \right) \leq C_{\text{LHS}}, \quad (5)$$

where $P(A_j = a)$ is the probability of the j -th measurement of Alice with outcome a , $\rho_a^{\hat{n}_j}(\theta, \phi) = |\chi_{\pm}^j(\theta, \phi)\rangle\langle \chi_{\pm}^j(\theta, \phi)|$ denote Bob’s projective measurements, C_{LHS} is the classical bound that determined by the maximal eigenvalue of the steering parameter $\mathcal{S}_k(\theta, \phi)$ for the given values of θ and ϕ .

The generated steering inequality (5) is a (θ, ϕ) -dependent inequality, one can use it to detect the steerability of two-qubit quantum states (pure or mixed). For the pure states given in Eq. (1), by choosing $\theta = \alpha$, $\phi = \varphi$, and due to $\sum_{a=0}^1 \text{tr}[(\hat{P}_a^{\hat{n}_j} \otimes \rho_a^{\hat{n}_j}) |\Psi\rangle\langle \Psi|] = \sum_{a=0}^1 \text{tr}(\tilde{\rho}_a^{\hat{n}_j}) = 1$, one can directly have the maximal violation as $\langle \Psi | \mathcal{S}_k | \Psi \rangle = k$.

Remarkably, the GLSI has two advantages over the usual LSI [20]: (i) Based on its own form as in (5), the GLSI includes naturally the usual LSI as a special case, thus can detect more quantum states. Especially, the GLSI can detect the steerability for all pure entangled states (1) in the whole region $\alpha \in (0, \pi/2)$, however, for the usual LSI, for some regions of α that closes to 0, it fails to detect the EPR steering. (ii) For the usual k -setting LSI, for different input states ρ_{AB} Bob needs to perform k measurements in different k directions, this is not very friendly for experiment because it is hard to tune accurately for all the k directions. However, the GLSI can overcome the disadvantage by the following operation: By using the Bloch realization $|\chi_{\pm}^j\rangle\langle \chi_{\pm}^j| = (\mathbb{1} + \vec{\sigma} \cdot \hat{n}_{\pm}^j)/2$, one can transform the GLSI to an equivalent form, where Bob only need to perform measurements along the \hat{x} , \hat{y} and \hat{z} directions, which is independent on the input states (see [19]). Therefore, it not only reduces the numbers of experimental

measurements, but also improves the experimental accuracy.

To be more specific, we give an example of the 3-setting GLSI from (5), where Alice’s three measuring directions are $\{\hat{x}, \hat{y}, \hat{z}\}$. Then we immediately have

$$\begin{aligned} \mathcal{S}_3 &= P(A_x = 0) \langle |\chi_+\rangle\langle \chi_+| \rangle + P(A_x = 1) \langle |\chi_-\rangle\langle \chi_-| \rangle \\ &\quad + P(A_y = 0) \langle |\chi'_+\rangle\langle \chi'_+| \rangle + P(A_y = 1) \langle |\chi'_-\rangle\langle \chi'_-| \rangle \\ &\quad + P(A_z = 0) \langle |0\rangle\langle 0| \rangle + P(A_z = 1) \langle |1\rangle\langle 1| \rangle \\ &\leq C_{\text{LHS}}, \end{aligned} \quad (6)$$

with $|\chi_{\pm}\rangle = \cos\theta|0\rangle \pm e^{i\phi}\sin\theta|1\rangle$, $|\chi'_{\pm}\rangle = \cos\theta|0\rangle \mp ie^{i\phi}\sin\theta|1\rangle$, $C_{\text{LHS}} = \text{Max}\{\frac{3+C_+}{2}, \frac{3+C_-}{2}\}$, and $C_{\pm} = \sqrt{4 \pm 4\cos 2\theta + \cos 4\theta}$. The equivalent 3-setting steering inequality is given by

$$\begin{aligned} \mathcal{S}'_3(\theta, \phi) &= \sin 2\theta \cos \phi \langle A_x \sigma_x \rangle - \sin 2\theta \cos \phi \langle A_y \sigma_y \rangle \\ &\quad + \sin 2\theta \sin \phi \langle A_x \sigma_y \rangle + \sin 2\theta \sin \phi \langle A_y \sigma_x \rangle \\ &\quad + \langle A_z \sigma_z \rangle + 2 \cos 2\theta \langle \sigma_z \rangle \leq C'_{\text{LHS}}, \end{aligned} \quad (7)$$

with $C'_{\text{LHS}} = \text{Max}\{C_+, C_-\}$. Obviously, by taking $\theta = \pi/4$, $\phi = 0$, the inequality (7) reduces to the usual 3-setting LSI in the following form [19][20]:

$$\mathcal{S}''_3(\theta, \phi) = \langle A_x \sigma_x \rangle - \langle A_y \sigma_y \rangle + \langle A_z \sigma_z \rangle \leq \sqrt{3}. \quad (8)$$

Quantum mechanically, Alice’s measurements will be represented as operators, such as $A_x \mapsto \sigma_x$, $A_y \mapsto \sigma_y$, $A_z \mapsto \sigma_z$. To test the GLSI in the experiment, Alice prepares two qubits and sends one of them to Bob, who trusts his own measurements but not Alice’s. Bob asks Alice randomly either to measure her qubit with σ_x , σ_y or σ_z , or simply not to perform any measurement; then Bob measures his qubit with σ_x , σ_y or σ_z according to Alice’s measurement. Finally, Bob obtains average values such as $\langle \sigma_x \otimes \sigma_x \rangle$, $\langle \sigma_y \otimes \sigma_y \rangle$, $\langle \sigma_x \otimes \sigma_y \rangle$, $\langle \sigma_y \otimes \sigma_x \rangle$, $\langle \sigma_z \otimes \sigma_z \rangle$, and $\langle \mathbb{1} \otimes \sigma_z \rangle$ and is therefore capable of checking whether the steering inequality (7) is violated or not. Particularly in the case of pure states (1), if Alice is honest in the preparation and measurements of the states, the inequalities will be violated within the entire region of α and φ (except at $\alpha = 0, \pi/2$), thereby confirming Alice’s ability to steer Bob.

Experiment results.—We shall experimentally demonstrate the steering paradox “2 = 1” and quantum violations of the GLSI via the photonic system. The experimental setup is shown in Fig. 1, the degenerated polarization-entangled photon pairs are created by pumping a 404nm laser to a type-II barium borate (BBO) crystal while the process of spontaneous parametric down-conversion occurs [21]. The initial two-photon state is a maximally entangled state $|\psi\rangle = (|HV\rangle - |VH\rangle)/\sqrt{2}$. To get the quantum state like (1), one should flip one of the qubits, add a relative phase between orthogonal state and redistribute the amplitude coefficients of the entangled state. Setting HWP1 at 0° can let the relative phase from “minus” to “plus”. And then, we utilize two half wave plate (HWP2 and HWP3) and beam displacers (BD) to construct an asymmetric loss interferometer. As shown in Fig. 1,

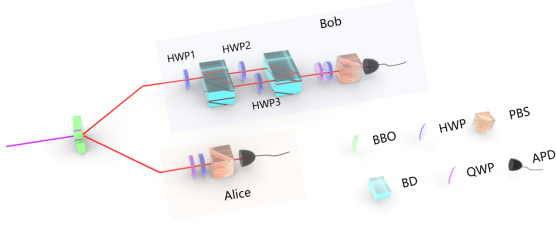


FIG. 1: **Experimental setup.** The polarization-entangled photons pairs are generated via type-II spontaneous parametric down-conversion. An asymmetric loss interferometer consisting of two beam displacers (BD) and half-wave plates (HWP) is implemented to prepare two-qubit pure entangled states. The projective measurements are performed using wave plates and polarization beam splitter (PBS).

Bob's photon passes through BD interferometer, HWP3 fixed at 45° and HWP2 at $\arcsin(\sqrt{\frac{1}{\sin^2 \alpha} - 1}) \cdot \frac{90}{\pi} \in [0, 45^\circ]$, which causes photon loss to adjust the amplitude and flips the qubit, to prepare desired two-qubit pure entangled state

$$|\Psi(\alpha)\rangle = \cos \alpha |HH\rangle + \sin \alpha |VV\rangle. \quad (9)$$

In this experiment, the phase φ in Eq. (1) is set to 0. The first qubit is sent to Alice, and the second to Bob. Alice and Bob measure their own photons through the polarization analyzer consisted of quarter-wave plate (QWP), HWP and PBS.

First, we come to test the EPR steering paradox “ $2 = 1$ ”. In our experiment, α is chosen from $\frac{\pi}{36}$ to $\frac{\pi}{4}$ with an interval of $\frac{\pi}{36}$ to obtain nine different two-qubit entangled states. In the two-setting steering scenario, Alice performs projective measurements along the \hat{x} -direction and \hat{z} -direction of Bloch sphere on her photons, respectively. The eigenvectors of σ_x are $|\pm\rangle = (|H\rangle \pm |V\rangle)/\sqrt{2}$, that is to say, the photon of Alice collapses into $|+\rangle$ or $|-\rangle$ in a certain probability. Meanwhile, the corresponding normalized conditional states for Bob become $|\chi_{\pm}\rangle = \cos \alpha |H\rangle \pm \sin \alpha |V\rangle$. Similarly, Bob's normalized conditional states are $|H\rangle$ and $|V\rangle$ when Alice perform σ_z operator with its eigenvector are $|H\rangle$ and $|V\rangle$. As shown in Fig. 2(a), the experimental results of quantum prediction S of nine different entangled pure states are far exceed the classical prediction. The average value of these quantum predictions is $S \approx 1.9899$, which is over 123 standard derivation of the classical value predicted by LHV models. Thus, the EPR paradox “ $2 = 1$ ” has been successfully demonstrated.

Second, we show the experimental result for violations of the GLSI by implementing the above state (9). We experimentally estimated the quantum value \mathcal{S}'_3 by using the 3-setting steering inequality (7). For simplicity, in our experiment the phase ϕ is chosen as 0, therefore, from (7) we only need to measure the following four observables: $\langle \sigma_x \otimes \sigma_x \rangle$, $\langle \sigma_y \otimes \sigma_y \rangle$, $\langle \sigma_z \otimes \sigma_z \rangle$, and $\langle \sigma_I \otimes \sigma_z \rangle$. Besides, in order to experimentally observe the violation of the GLSI for any $\alpha \in (0, \pi/4]$, for a fixed α we need to maximize the difference between quantum value \mathcal{S}'_3 and classical bound C'_{LHS} by

numerically solving the optimal solutions of θ . Notably, when $\alpha \in (0, (\arcsin \frac{\sqrt{3}-1}{2})/2 \approx \frac{\pi}{17}]$, we observed a significant violation that is impossible for the usual 3-setting LSI (8). When α is close to $\pi/4$, the violation behaviors of the GLSI (7) and the LSI (8) are almost the same. The experimental results are shown in Fig. 2(b), which are coincidence with the theoretical results.

Third, we also experimentally test the inequality (7) with two types of mixed states [19]. The first one is the generalized Werner state ρ_1 , and the second one is an asymmetric mixed state ρ_2 given in [22]:

$$\rho_1 = V |\Psi(\alpha)\rangle \langle \Psi(\alpha)| + \frac{1-V}{4} \mathbb{1} \otimes \mathbb{1}, \quad (10a)$$

$$\rho_2 = V |\Psi(\alpha)\rangle \langle \Psi(\alpha)| + (1-V) |\Phi(\alpha)\rangle \langle \Phi(\alpha)|, \quad (10b)$$

with $|\Phi(\alpha)\rangle = \sin \alpha |HV\rangle + \cos \alpha |VH\rangle$, $\alpha \in [0, \frac{\pi}{4}]$, and $V \in [0, 1]$. As shown in Fig. 2(c), the experimental points of the generalized Werner states are fitted with theoretical quantum values. Meanwhile, the zoom area is the obvious area that cannot be observed in usual LSI, while we can observe some steering evidences even in this area by the GLSI. We further prepare the mixed state ρ_2 to experimentally verify the superiority of the GLSI. The experimental results are shown in the Fig. 2(d) and we make the same conclusion that the GLSI can detect steering in a more expansive quantum state space. The more detail analysis are presented in Supplementary Information [19].

Conclusions.—In conclusion, we have advanced the study of EPR paradox: (i) We have made the first observation of the simplest EPR paradox “ $2 = 1$ ” in a two-qubit system, the experimental result coincides with the theoretical one. (ii) Based on the more general EPR paradox “ $k = 1$ ”, we have successfully derived the k -setting generalized linear steering inequality, which can detect more steerability of quantum states than the previous ones. Importantly, we find that the inequality can be transformed into a mathematically equivalent form, which is more friendly for experimental implementation. The equivalent form of steering inequality suffices in our experiment to measure only along the x -, y -, or z -axis in Bloch's sphere, rather than other arbitrary directions, thus greatly simplifying the experimental setups and reducing experimental deviations. This finding is also very valuable for an open problem how to optimize the measurement settings of steering verification in experiments, which has been specially pointed out in [23]. Finally, it is a challenge to experimental demonstrate the EPR paradox with the original EPR state $\Psi(x_1, x_2)$ in an entangled continuous-variable system, we anticipate the experimental progress in this direction in the near future.

This work is supported by the National Key Research and Development Program (2017YFA0305200 and 2016YFA0301700), the Key Research and Development Program of Guangdong Province of China (2018B030329001 and 2018B030325001) and the Natural Science Foundation of Guangdong Province of China (2016A030312012). X.Z. acknowledges support from the National Young 1000 Talents Plan. C.R. is supported by Youth Innovation Pro-

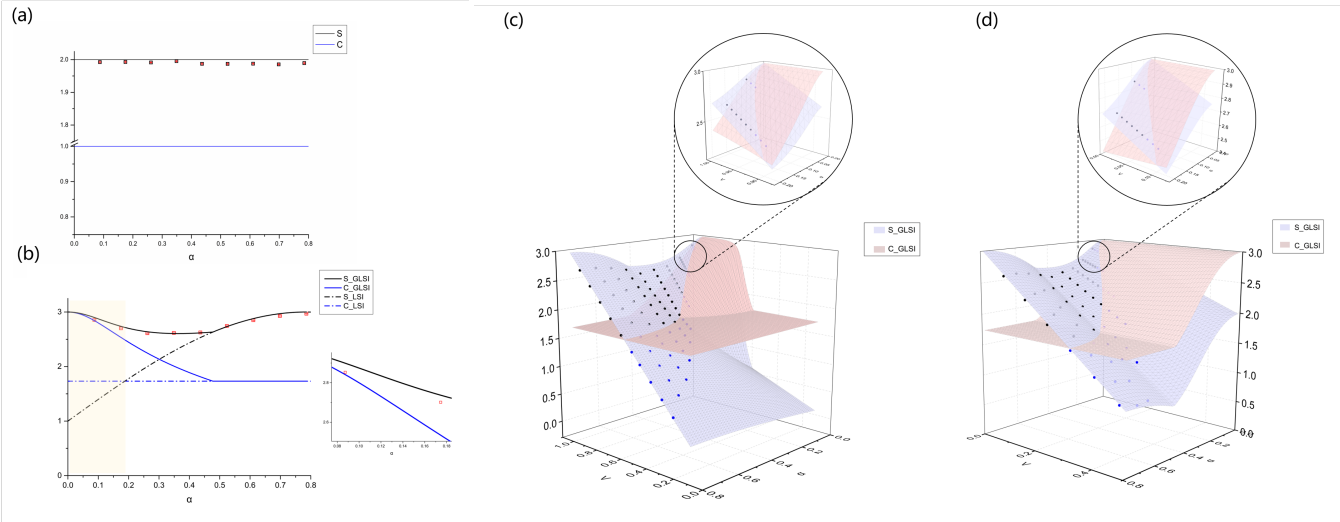


FIG. 2: **The experimental results for pure states.** (a) shows the experimental result of the EPR paradox “2=1”. The black and blue solid lines represent the quantum prediction $S \equiv P_{\text{total}}^{\text{QM}} = 2$ and the classical prediction $C = 1$ based on the LHV models, respectively. The black cubes and inserting red lines show the experimental results with error bar. (b) shows the experimental results for the 3-setting GLSI (7). The black and blue solid line represent the quantum and classic values, respectively, which are the optimal numerical solutions for maximizing the difference between quantum value S'_3 and classical bound C'_{LHS} for a fixed α . The black (blue) dot line represents the quantum violations ($S'_3 = 1 + 2 \sin(2\alpha)$) (the classical value $C = \sqrt{3}$) of the usual 3-setting LSI (8), respectively. The red cubes are the experimental points implementing the inequality (7). The light yellow range is $\alpha \in (0, (\arcsin \frac{\sqrt{3}-1}{2})/2]$, which the LSI (8) cannot detect the steerability but the GLSI can. The right inset shows the experimental results of $\alpha = \frac{\pi}{36}, \frac{\pi}{18}$ for the clear observation. **The experimental results for mixed states.** (c) and (d) show the steering detection based on the simplified Pauli measurements for the generalized Werner state and an asymmetric mixed state. The light purple and pink curved surface represent the quantum value and the classical bound of the GLSI (7), respectively. The black (blue) dots represent the quantum states that can (cannot) experimentally violate the GLSI (7). The zoom area is the obvious area that cannot be observed in usual LSI (8), while one can observe some steering evidences even in this area by the GLSI (7).

motion Association (CAS) No. 2015317, Natural Science Foundations of Chongqing (No.cstc2013jcyjC00001, cstc2015jcyjA00021) and The Project-sponsored by SRF for ROCS-SEM (No.Y51Z030W10). J.L.C. is supported by National Natural Science Foundations of China (Grant No. 11875167). T.F., C.R. and Q.F. contributed equally to this work.

* Electronic address: renchangliang@cigit.ac.cn

† Electronic address: chenjl@nankai.edu.cn

‡ Electronic address: zhouxq8@mail.sysu.edu.cn

- [1] A. Einstein, B. Podolsky, and N. Rosen, Phys. Rev. **47**, 777 (1935).
- [2] D. M. Greenberger, M. A. Horne, and A. Zeilinger, in *Bell's Theorem, Quantum Theory, and Conceptions of the Universe*, edited by M. Kafatos (Kluwer, Dordrecht, 1989), p. 69.
- [3] L. Hardy, Phys. Rev. Lett. **71**, 1665 (1993).
- [4] E. Schrödinger, Naturwiss. **23**, 807 (1935).
- [5] H. M. Wiseman, S. J. Jones, and A. C. Doherty, Phys. Rev. Lett. **98**, 140402 (2007).
- [6] J. S. Bell, Physics (Long Island City, N.Y.) **1**, 195 (1964).
- [7] N. Brunner, D. Cavalcanti, S. Pironio, V. Scarani, and S. Wehner, Rev. Mod. Phys. **86**, 419 (2014).
- [8] J. Clauser, M. Horne, A. Shimony, and R. Holt, Phys. Rev. Lett. **23**, 880 (1969).

- [9] N. D. Mermin, Phys. Rev. Lett. **65**, 1838 (1990).
- [10] D. Collins, N. Gisin, N. Linden, S. Massar, and S. Popescu, Phys. Rev. Lett. **88**, 040404 (2002).
- [11] A. Aspect, P. Grangier, and G. Roger, Phys. Rev. Lett. **47**, 460 (1981).
- [12] J. W. Pan, D. Bouwmeester, M. Daniell, H. Weinfurter, and A. Zeilinger, Nature (London) **403**, 515 (2000).
- [13] J. R. Torgerson, D. Branning, C. H. Monken, and L. Mandel, Phys. Lett. A **204**, 323 (1995).
- [14] J. R. Torgerson, D. Branning, C. H. Monken, and L. Mandel, Phys. Lett. A **204**, 323 (1995).
- [15] Y. H. Luo *et al.*, Sci. Bull. **63**, 1611 (2018).
- [16] J. L. Chen, H. Y. Su, Z. P. Xu, and A. K. Pati, Sci. Rep. **6**, 32075 (2016).
- [17] N. D. Mermin, Am. J. Phys. **62**, 880 (1994).
- [18] S. H. Jiang, Z. P. Xu, H. Y. Su, A. K. Pati, and J. L. Chen, Phys. Rev. Lett. **120**, 050403 (2018).
- [19] See the Supplementary Information.
- [20] D. J. Saunders, S. J. Jones, H. M. Wiseman, and G. J. Pryde, Nat. Phys. **6**, 845-849 (2010).
- [21] P.G. Kwiat, K. Mattle, H. Weinfurter, and A. Zeilinger, Phys. Rev. Lett. **75**, 4337 (1995).
- [22] J. L. Chen, X. J. Ye, C. Wu, H. Y. Su, A. Cabello, L. C. Kwek, and C. H. Oh, Sci. Rep. **3**, 02143 (2013).
- [23] R. Uola, A. C. S. Costa, H. C. Nguyen, and O. Gühne, Rev. Mod. Phys. **92**, 015001 (2020).